

Size effect on the crystal phase of cobalt fine particles

Osamu Kitakami,* Hisateru Sato, and Yutaka Shimada

*Section of Solid State Electron Physics, Research Institute for Scientific Measurements, Tohoku University,
2-1-1 Katahira, Aoba, Sendai 980-77, Japan*

Futami Sato and Michiyoshi Tanaka

*Section of Surface Science, Research Institute for Scientific Measurements, Tohoku University,
2-1-1 Katahira, Aoba, Sendai 980-77, Japan*

(Received 30 June 1997)

We have synthesized Co fine particles with the average diameter (D) of less than 500 Å by sputtering Co in a somewhat high inert-gas pressure. It has been found that there is a close relationship between the particle size and the crystal phase; that is, pure fcc (β) phase for $D \leq 200$ Å, a mixture of hcp (α) and β phases for $D \sim 300$ Å, and α phase with inclusion of a very small amount of β phase for $D \geq 400$ Å. Precise structural characterizations have revealed that the β particles are multiply twinned icosahedrons and the α particles are perfect single crystals with external shape of a Wulff polyhedron. In order to explain the size effect on the crystal phase of Co fine particles, we have performed theoretical calculations for total free energies of an α single crystal, a β single crystal, and a multiply twinned β icosahedron. The present calculations well explain the size dependence of the crystal phase of the Co fine particles, and have revealed that the stabilization of β phase, confirmed by previous studies, is the intrinsic effect caused by the small dimensionality of fine particles. Moreover, the phase transformations that occurred in annealing experiments can also be explained by the theory. [S0163-1829(97)05145-X]

INTRODUCTION

Numerous studies in the past five decades have revealed that fine particles of several elements often show anomalies in the phase transformation and the phase stability, resulting in metastable and unique crystal phase quite different from bulk specimens.¹⁻⁸ For example, Cr particles as small as several hundreds of nanometers exhibit an abnormal A15 metastable phase that has been later found as a high-temperature phase in bulk form.⁸⁻¹⁰ Analogous behavior has been found also for Co,^{1-3,7,8,11} where the particles always crystallize in the high-temperature fcc phase that is only stable above 420 °C in bulk form.¹² The origin of such an unusual behavior found in Co still remains ambiguous in spite of intensive efforts. Some authors have speculated that the high-temperature face-centered cubic (fcc) phase appeared as a metastable state as a consequence of rapid cooling in the growth process of the fine particles.^{7,8} According to our recent experiments, Co fine particles with a diameter of 10 nm prepared by sputtering also have a pure fcc phase, and subsequent annealing above the bulk fcc (β)-hcp (α) transformation temperature and very slow cooling to ambient temperature do not cause any phase changes.¹³ Therefore, it is unlikely that the β phase is simply produced as a nonequilibrium state by rapid cooling in the fine particle growth process. Moreover, the allotropic $\beta \rightarrow \alpha$ transformation is entirely inhibited down to 28 K, thus the β phase seems to be energetically stable.¹⁴ In a previous paper, we have reported success in the synthesis of α -Co fine particles with a diameter of about 40 nm, and found the close relationship between the crystal phase and the particle size.¹⁴

The aim of the present study is to explore the phase stability of α - and β -Co fine particles and to discuss the particle

size effect on the crystal phase from the standpoint of the total free energy including surface free energy.

EXPERIMENT

Fine Co particles were prepared in a homemade dc magnetron sputtering system at ambient temperature, with a base pressure less than 1×10^{-7} Torr and argon gas pressure (P_{Ar}) of 0.1–0.5 Torr. The details of the sputtering apparatus and the experimental conditions are described elsewhere.¹³⁻¹⁵ Annealing of the particles was performed in vacuum of $\sim 1 \times 10^{-6}$ Torr at various temperatures. Particle size and shape were checked by transmission electron microscopy (TEM) and scanning electron microscopy (SEM). The crystal structures of the Co particles were examined by means of x-ray diffraction (XRD) with Cu- $K\alpha$ line and selected area electron diffraction. In the x-ray diffraction experiments, no distinct diffractions other than those from α - and β -Co were found in all samples prepared in the present study. The pole figure measurements of $\alpha(10\bar{1}0)$, (0002) , $(10\bar{1}1)$, and $\beta(111)$, (200) reflections have revealed three-dimensionally random orientation of the particles. For random orientation, integrated diffraction intensity is given by

$$I = C \left(\frac{1}{\nu^2} \right) \left[|F|^2 p \left(\frac{1 + \cos^2 2\theta}{\sin^2 \theta \cos \theta} \right) \right] \left(\frac{e^{-2M}}{2\mu} \right), \quad (1)$$

where C is a constant determined by measurement conditions, ν the volume of a unit cell, $|F|$ the structure factor, p the multiplicity factor, θ the Bragg angle, e^{-2M} the Debye temperature factor, and μ the linear absorption coefficient.¹⁶ For the mixture of α and β phases, the diffraction intensity can be simply expressed as

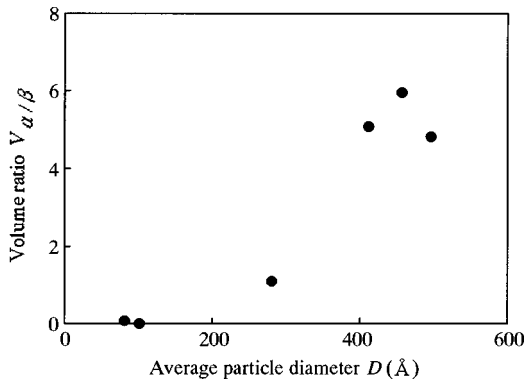


FIG. 1. Particle size dependence of volume ratio of hcp (α -) to fcc (β -) phase $V_{\alpha/\beta}$ for Co fine particles. It is clearly noted that α -phase becomes dominant with increase in the particle diameter D .

$$I_{\text{mix}}(\theta) = \sum_{\alpha, \beta} c_i I_i(\theta), \quad (2)$$

where c_i and I_i are the volume fraction and the diffraction intensity. Using Eqs. (1) and (2), we can calculate relative intensity ratios of all diffractions from both α and β phases as a function of the volume fractions. It was found that the relative intensities calculated by the above equations can be well fitted to all experimental data by varying the volume fraction of α phase (c_α). Thus, we can determine the volume ratio of α phase to β phase as $V_{\alpha/\beta} = c_\alpha/c_\beta = c_\alpha/(1-c_\alpha)$. The fitting procedures were performed for $\alpha(10\bar{1}0)$, (0002) , $(10\bar{1}1)$, and $\beta(111)$, (200) .

RESULTS AND DISCUSSION

In the previous paper, the particle size and the crystal phase of Co were found to be considerably influenced by their growth conditions.¹⁴ That is, the increase in the sputtering gas pressure increased the particle size as well as the

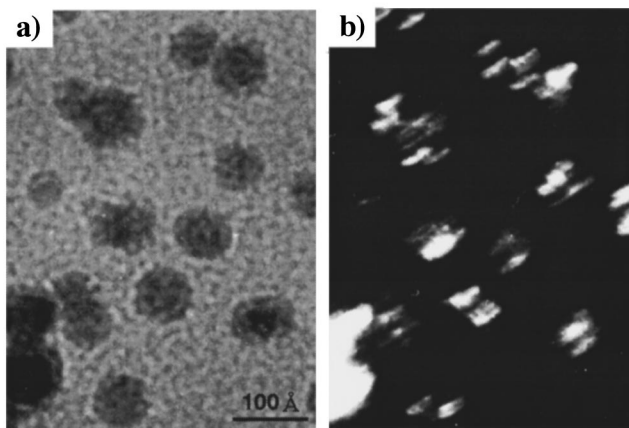


FIG. 2. TEM micrographs of the pure β -Co particles ($V_{\alpha/\beta} = 0$) grown at Ar gas pressure of 0.15 Torr, (a) the bright field image, and (b) the corresponding dark field image formed by $\beta(111)$ diffraction spots. Each particle exhibits a butterflylike contrast in the dark field image.

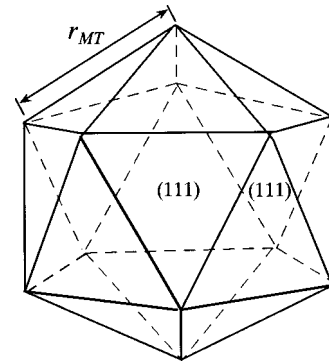


FIG. 3. A multiply twinned (MT) icosahedron composed of twenty tetrahedrons each of which is surrounded by four $\beta(111)$ faces. The icosahedron consists of one nucleus, three primary, six secondary, six tertiary, three quartic, and one quintic twins (Ref. 17).

preferential growth of α phase instead of β phase, and there is a close relationship between the particle size and the crystal phase.¹⁴ From Fig. 1, the crystal phase apparently depends on the particle size (D): namely, pure β phase for $D \leq 200$ Å, mixture of α and β phases for $D \sim 300$ Å, and α phase with inclusion of a small amount of β phase for $D \geq 400$ Å. Detailed structural analyses have revealed that most particles prepared in the present study possess well-defined crystal habits and structures. Figures 2(a) and 2(b) show the bright and the dark field images of pure β particles ($V_{\alpha/\beta} = 0$) grown at $P_{\text{Ar}} = 0.15$ Torr. The dark field image was formed using $\beta(111)$ diffraction spots. From these figures, it can be noticed that most particles exhibit butterflylike contrasts in the dark field image as shown in Fig. 2(b). Previous studies have revealed that such image contrasts can be well explained by the multiply twinned (MT) icosahedrons that are commonly observed in various fine particles with a fcc structure¹⁷ (Fig. 3). In fact, the diffraction pattern from the each particle perfectly coincides with that of the multiply twinned icosahedron originally pointed out by Ino¹⁷ (Fig. 4). Thus, we can safely conclude that very fine β particles smaller than 100 Å mainly consist of MT icosahedral particles. This result agrees well with the previous theoretical prediction that states that MT icosahedron is energetically stable for very small fcc particles.¹⁸ With increasing the sputtering gas pressure, the particle size increases and the α phase becomes dominant, as shown in Fig. 1. Figures 5(a) and 5(b), respectively, show the bright and the dark field

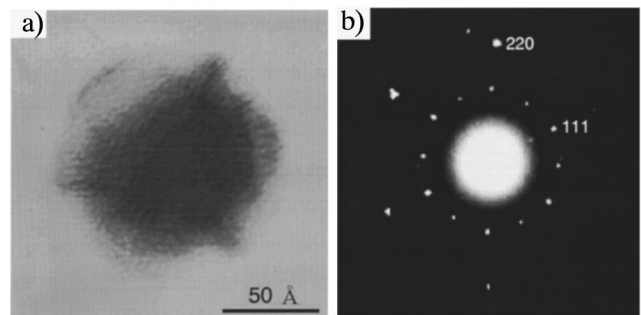


FIG. 4. (a) A bright field image and (b) the corresponding diffraction pattern of a MT icosahedron particle.

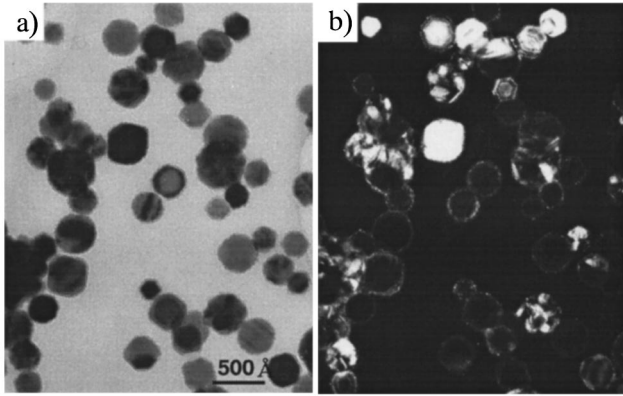


FIG. 5. TEM micrographs of α -Co particles with inclusion of a small amount of β particles ($V_{\alpha/\beta}=5$) prepared at Ar gas pressure of 0.35 Torr, (a) the bright field image, and (b) the corresponding dark field image formed by portion of $\alpha(0002)$ and $(10\bar{1}1)$ diffraction spots. Each particle possesses a well-defined crystal habit and seems to be single crystal.

images of nearly pure α -Co particles ($V_{\alpha/\beta}=7$) grown at $P_{Ar}=0.35$ Torr. The dark field image was formed using a portion of $\alpha(10\bar{1}0)$, (0002) , and $(10\bar{1}1)$ diffraction spots. It can be clearly noticed that most particles possess well-defined crystal habits and seem to be single crystals. Their external shapes [Fig. 6(a)] coincide well with the Wulff polyhedron of α -Co [Fig. 6(b)] constructed by the following Gibbs-Wulff relation:¹⁹

$$\sum \gamma_i S_i = \text{minimum}, \quad (3)$$

where γ_i is the specific surface free energy of the i th crystal face whose surface area is S_i . Furthermore, the high resolution TEM observations and the corresponding diffractions have revealed that each α -Co particle is an exactly pure single crystal. Figures 7(a)–(c) are, respectively, the bright field image, the enlarged lattice image, and the corresponding diffraction pattern taken along $[0001]$ of the α particle. Thus, the particles prepared at somewhat high sputtering gas pressure are α -Co single crystals, although stacking faults are sometimes included in the α particles.

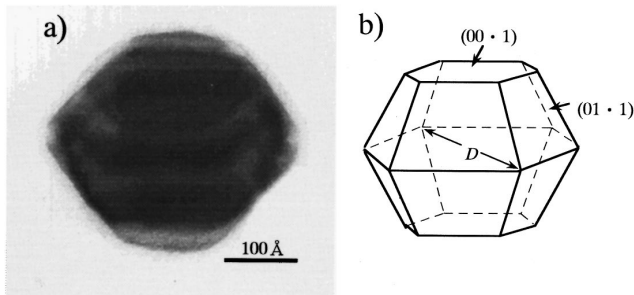


FIG. 6. (a) An external shape of an α -Co particle grown at Ar gas pressure of 0.35 Torr, and (b) the Wulff polyhedron of α -Co constructed by the Gibbs-Wulff relation. Both external shapes look very similar.

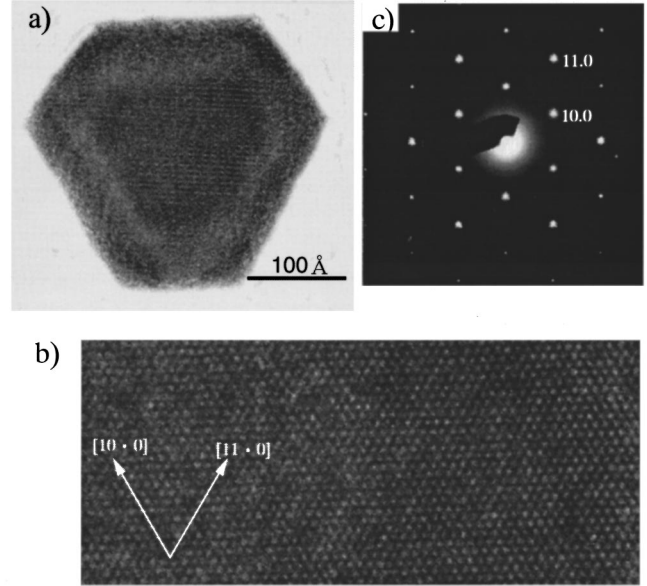


FIG. 7. (a) A bright field image, (b) the lattice image, and (c) the electron-diffraction pattern taken along $[0001]$ of an α -Co particle grown at Ar gas pressure of 0.35 Torr. These results indicate that the particle is a perfect α single crystal.

In order to investigate the phase stabilities of the above α and β particles, we performed annealing experiments at various temperatures. Figure 8 shows the change in the volume ratio $V_{\alpha/\beta}$ as a function of annealing temperature (T_a) for Co particles ($V_{\alpha/\beta}=3.5$, average particle diameter $D\sim 300$ Å). As can be noticed in this figure, $V_{\alpha/\beta}$ slightly increases and then abruptly decreases with increase in annealing temperature. This result indicates that $\beta\rightarrow\alpha$ transformation proceeds at low annealing temperature and then the reverse transformation ($\alpha\rightarrow\beta$) occurs at higher temperature. For a pure β sample ($V_{\alpha/\beta}=0$), XRD measurements showed that the diffraction peak from $\beta(111)$ becomes sharp abruptly as T_a exceeds 300 °C. This change is not due to coalescence of β particles but due to the fact that multiply twinned β particles transform into single crystals. In fact, a lot of β single-crystal

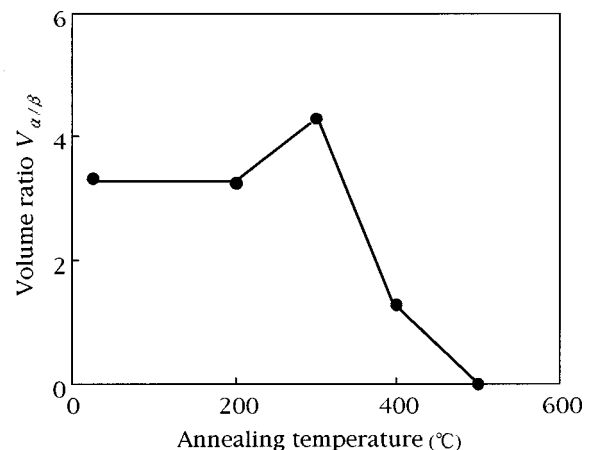


FIG. 8. Variation of volume ratio $V_{\alpha/\beta}$ as a function of annealing temperature (T_a).

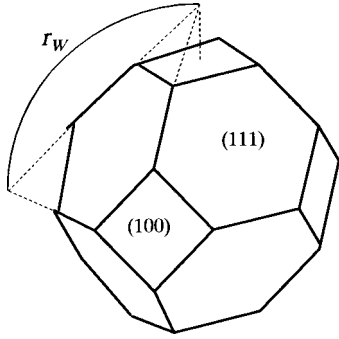


FIG. 9. A β -Wulff polyhedron surrounded by eight (111) and six (100) faces, which satisfies the Gibbs-Wulff relation Eq. (3) in the text.

particles with ideal Wulff polyhedral shape (Fig. 9) were found in those annealed samples, as shown in Figs. 10(a) and 10(b).

We discuss the particle size effect on crystal phase and stability of Co fine particles. The total free energy for an α particle with the Wulff polyhedron shape shown in Fig. 6(a) can be expressed as

$$U_{\text{Wulff-}\alpha} = -U_{c-\alpha} + U_{s-\alpha} + U_{sf}, \quad (4)$$

where $U_{c-\alpha}$, $U_{s-\alpha}$, and U_{sf} denote the cohesive energy, the surface energy, and the stacking fault energy, respectively. Since stacking faults parallel to the (0001) plane were frequently observed in the α -Co particles, we added the third term, although this term is trivial compared with the other terms. The energy terms in Eq. (4) are given by

$$U_{c-\alpha} = E_{c-\alpha} V_{\alpha}(D), \quad (5)$$

$$U_{s-\alpha} = \gamma_{00\cdot1} \sum S_{00\cdot1} + \gamma_{01\cdot1} \sum S_{01\cdot1}, \quad (6)$$

$$U_{sf} = \gamma_{sf} \sum S_{sf}, \quad (7)$$

where $E_{c-\alpha}$ is the cohesive energy of α -Co per unit volume, $V_{\alpha}(D)$ is the volume of the Wulff polyhedron in Fig. 6(a) and can be calculated as $0.409D^3$, $\gamma_{hk\cdot l}$ is the surface energy

of $(hk\cdot l)$ plane, $S_{hk\cdot l}$ is the surface area of each $(hk\cdot l)$ plane, γ_{sf} is the stacking fault energy per unit area, and S_{sf} is the surface area of each stacking fault plane. Assuming that each α -Co particle contains seven stacking fault planes in it, the total area can be derived as $\sum S_{sf} = 6.93D^2$. This assumption gives rise to no serious errors, since the third energy term in Eq. (4) is trivial compared with the other terms. In evaluating the energy terms in Eqs. (5) and (7), we used the bulk values of α -Co for $E_{c-\alpha}$ (Ref. 20) and γ_{sf} .²¹ For evaluation of the surface energies in Eq. (6), we adopted the theoretical values determined by a spin-polarized Green's function method,²² which almost agree with experiments²³ and the thermodynamically estimated values.²⁴ On substituting these values into Eqs. (5)–(7), Eq. (4) can be rewritten as

$$\begin{aligned} U_{\text{Wulff-}\alpha} &= -E_{c-\alpha} V_{\alpha}(D) + 9.56 \times 10^{-20} D^2 + 0.16 \times 10^{-20} D^2 \\ &= -E_{c-\alpha} V_{\alpha}(D) + 9.72 \times 10^{-20} D^2 \quad (\text{Joule}). \end{aligned} \quad (8)$$

Here, D is in angstroms. Similarly, the total energy for a β -Wulff polyhedron shown in Fig. 9 can be expressed as

$$\begin{aligned} U_{\text{Wulff-}\beta} &= -U_{c-\beta} + U_{s-\beta} \\ &= -E_{c-\beta} V_{\beta}(r_w) + \gamma_{111} \sum S_{111} + \gamma_{100} \sum S_{100}, \end{aligned} \quad (9)$$

where $E_{c-\beta}$ is the cohesive energy of β -Co per unit volume, $V_{\beta}(r_w)$ is the volume of the polyhedron and is given by $V_{\beta}(r_w) = 0.377r_w^3$. Under the condition of $V_{\alpha}(D) = V_{\beta}(r_w)$, r_w is equal to $1.03D$. Since there is the slight difference in free energies between α - and β -Co at room temperature, the first term in Eq. (9) is rewritten as

$$-E_{c-\beta} = -E_{c-\alpha} + \Delta E_{\beta-\alpha}, \quad (10)$$

where $\Delta E_{\beta-\alpha}$ is the free energy difference estimated to be 0.06 kcal/mol.²⁵ The total energy of the β -Wulff polyhedron in Eq. (9) can be derived as

$$\begin{aligned} U_{\text{Wulff-}\beta} &= -E_{c-\alpha} V_{\beta}(r_w) + \Delta E_{\beta-\alpha} V_{\beta}(r_w) + \gamma_{111} \sum S_{111} \\ &\quad + \gamma_{100} \sum S_{100} \\ &= -E_{c-\alpha} V_{\beta}(r_w) + 1.54 \times 10^{-23} D^3 + 7.97 \\ &\quad \times 10^{-20} D^2 \quad (\text{Joule}). \end{aligned} \quad (11)$$

Here we used the theoretical surface energy values determined by the spin-polarized Green's function method.²² Next, we consider the total energy of a β -MT icosahedron shown in Fig. 3. In this case, both the elastic strain energy U_e and the twin boundary energy U_t are added to the total energy of Eq. (9). Therefore, the total energy is given by

$$\begin{aligned} U_{\beta\text{-MT}} &= -U_{c\text{-MT}} + U_{s\text{-MT}} + U_e + U_t \\ &= -E_{c-\beta} V_{\text{MT}}(r_{\text{MT}}) + \gamma_{111} \sum S_{111} + U_e + U_t, \end{aligned} \quad (12)$$

where $V_{\text{MT}}(r_{\text{MT}})$ is the volume of the MT icosahedron and is given by $V_{\text{MT}}(r_{\text{MT}}) = 5\sqrt{2}/3r_{\text{MT}}^3$, and $\sum S_{111} = 5\sqrt{3}r_{\text{MT}}^2$. Under the condition of $V_{\alpha}(D) = V_{\text{MT}}(r_{\text{MT}})$, r_{MT} is equal to $0.558D$. If we assume uniform straining in the particle, the elastic strain energy U_e in Eq. (12) is given by

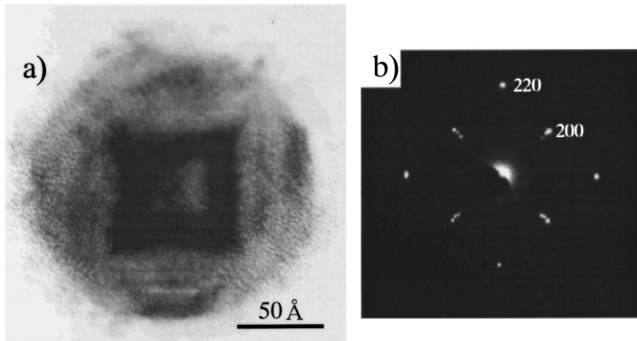


FIG. 10. (a) A bright field image and (b) the corresponding diffraction pattern taken along [001] of a β -Wulff polyhedron. We note that the particle is a perfect β -single crystal and its external shape well coincides with the Wulff polyhedron shown in Fig. 9.

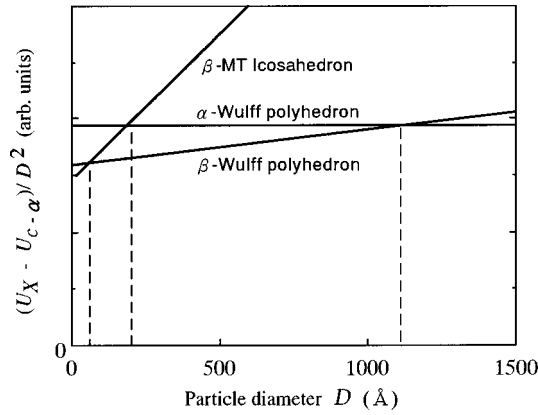


FIG. 11. Calculated energy diagram of a Co fine particle as functions of particle diameter D for three different crystalline states, that is, a β -MT icosahedron, a β -Wulff polyhedron, and an α -Wulff polyhedron. In this figure, the suffix X stands for β -MT, β -Wulff, and α -Wulff, and the $U_{c-\alpha}$ represents the cohesive energy of an α -Co particle. It can be noticed that β phase becomes more stable than α -phase as the particle size reduces.

$$U_e = V_{\text{MT}}(r_{\text{MT}})E_e = 5\sqrt{2}/3r_{\text{MT}}^3E_e, \quad (13)$$

where E_e is the strain energy per unit volume. Ino¹⁸ accurately calculated the strain energy and obtained $E_e = 28.1 \times 10^7 \text{ J/m}^3$ for the β -MT icosahedron. The twin boundary energy U_t in Eq. (12) is given by

$$U_t = \gamma_{\text{twin}} \Sigma S_{\text{twin}} = 15\sqrt{3}/2r_{\text{MT}}^2 \gamma_{\text{twin}}, \quad (14)$$

where γ_{twin} denotes the energy per unit area and is evaluated as $\gamma_{\text{twin}} = 4.5 \times 10^{-3} \text{ J/m}^2$.²⁶ On substituting Eqs. (10), (13), and (14) into Eq. (12), the total energy for the β -MT icosahedron can be expressed as

$$U_{\beta\text{-MT}} = -U_{c-\alpha} + 13.0 \times 10^{-23} D^3 + 7.29 \times 10^{-20} D^2 \quad (\text{Joule}). \quad (15)$$

From Eqs. (8), (11), and (15), we can calculate and compare the total free energies of an α -Wulff polyhedron, a β -Wulff polyhedron, and a β -multiply twinned icosahedron as a function of particle size. Calculated results are shown in Fig. 11. It can be noticed that both a β -MT icosahedron and a β -Wulff polyhedron are energetically more stable than an α -Wulff polyhedron for particle sizes of less than 200 Å. This fact means that fine Co particles prefer β phase to α phase, and well explains numerous experimental results so far obtained as well as the present result shown in Fig. 1. Such an unusual behavior found in Co fine particles comes from an intrinsic size effect. That is, a slightly smaller surface free

energy of β -Co causes preferential growth of β phase for a very small size region. In contrast, α phase becomes predominant as the particle size increases, because contribution of the surface free energy reduces with increase of particle size. We note from Fig. 11 that the relationships of the three energy levels $U_{\text{Wulff-}\beta}$, $U_{\beta\text{-MT}}$, and $U_{\text{Wulff-}\alpha}$ are given as

$$U_{\text{Wulff-}\beta} \leq U_{\beta\text{-MT}} < U_{\text{Wulff-}\alpha} \quad \text{for } 60 \leq D < 180 \text{ \AA},$$

$$U_{\text{Wulff-}\beta} < U_{\text{Wulff-}\alpha} \leq U_{\beta\text{-MT}} \quad \text{for } 180 \leq D < 1100 \text{ \AA},$$

$$U_{\text{Wulff-}\alpha} \leq U_{\text{Wulff-}\beta} < U_{\beta\text{-MT}} \quad \text{for } D \geq 1100 \text{ \AA}.$$

Since a β -MT icosahedron is the intermediate energy state for $60 \leq D < 180 \text{ \AA}$, the β -MT icosahedron particles found in Figs. 2 and 4 are considered to be metastable. In fact, they transform into the most stable β -Wulff polyhedrons by annealing treatment (Fig. 10). For the Co particle samples with average diameter of $D \geq 180 \text{ \AA}$, α -Wulff polyhedron particles are dominant with inclusion of a certain amount of β particles, as can be noticed in Figs. 5–7. They exhibit $\beta \rightarrow \alpha$ transformation at low annealing temperature $T_a \leq 300 \text{ }^\circ\text{C}$ and subsequently $\alpha \rightarrow \beta$ transformation occurs at higher T_a (Fig. 8). Such an unusual transformation behavior can be explained if we assume that the β particles included in the as-made samples are β -MT icosahedrons. According to Fig. 11, β -MT icosahedrons possess higher energy than α -Wulff polyhedrons, hence annealing will cause $\beta \rightarrow \alpha$ transformation, resulting in a slight increase in volume fraction of α phase. Finally, all these α particles will transform into the lowest-energy state, namely, β -Wulff polyhedrons at higher T_a .

As mentioned above, we can understand most of the present experiments and other previous experimental results based on simple considerations of particle free energy. However, the present discussions can give no clear answers to the question why as-made Co fine particles favor metastable states (such as multiply twinned icosahedrons or α -Wulff polyhedrons) instead of the more energetically favorable β -Wulff polyhedrons. In order to answer this question, we have to elucidate the dynamics of each phase transformation that has occurred in Co fine particles as well as quantitative evaluation of the activation energy required for each phase transformation.

ACKNOWLEDGMENTS

The authors sincerely thank K. Fukamichi for invaluable discussions, T. Sakurai for technical assistance, and H. Daimon and K. Adachi for performing some TEM observations. This work was supported by RFTF of Japan Society for the Promotion of Science under Grant No. 97R14701 and Grant-in-Aid from the Ministry of Education, Science, and Culture under Grant No. 08650763.

*Author to whom correspondence should be sent. Electronic address: kitakami@rism.tohoku.ac.jp FAX: +81-22-217-5404.

¹O. S. Edwards and H. Lipson, Proc. R. Soc. London, Ser. A **180**, 268 (1943).

²A. R. Troiano and J. L. Tokich, Trans. Metall. Soc. AIME **195**, 728 (1948).

³E. A. Owen and D. M. Jones, Proc. R. Soc. London, Ser. B **67**, 456 (1954).

⁴R. E. Cech and D. Turnbull, J. Met. **8**, 124 (1956).

⁵W. C. Leslie and R. L. Miller, Trans. ASM **57**, 972 (1964).

⁶Y. Fukano, Jpn. J. Appl. Phys. **13**, 1001 (1974).

⁷C. G. Granqvist and R. A. Buhrman, J. Appl. Phys. **47**, 2200

- (1976).
- ⁸K. Kimoto and I. Nishida, *J. Phys. Soc. Jpn.* **22**, 744 (1967).
- ⁹N. Yukawa, M. Hida, T. Imura, M. Kawamura, and Y. Mizuno, *Metall. Trans. A* **3**, 887 (1972).
- ¹⁰C. Panzera, R. C. Krutenat, and M. J. Donachie, Jr., *J. Vac. Sci. Technol.* **8**, VM80 (1971).
- ¹¹S. Gangopdhyay, G. C. Hadjipanayis, S. M. Sorensen, and K. J. Klabunde, *IEEE Trans. Magn.* **28**, 3174 (1992); J. P. Chen, C. M. Sorensen, K. J. Klabunde, and G. C. Hadjipanayis, *J. Appl. Phys.* **76**, 6316 (1994); E. Anno, *Phys. Rev. B* **50**, 17 502 (1994); J. Jiao, S. Seraphin, X. Wang, and J. C. Withers, *J. Appl. Phys.* **80**, 103 (1996), and references therein.
- ¹²M. Hansen, *Constitution of Binary Alloys* (McGraw-Hill, New York, 1958).
- ¹³O. Kitakami, T. Sakurai, Y. Miyashita, Y. Takeno, Y. Shimada, H. Takano, H. Awano, and Y. Sugita, *Jpn. J. Appl. Phys.* **35**, 1724 (1996).
- ¹⁴H. Sato, O. Kitakami, T. Sakurai, Y. Shimada, Y. Otani, and K. Fukamichi, *J. Appl. Phys.* **81**, 1858 (1997).
- ¹⁵T. Sakurai, O. Kitakami, and Y. Shimada, *J. Magn. Magn. Mater.* **130**, 384 (1994); O. Kitakami, T. Sakurai, and Y. Shimada, *J. Appl. Phys.* **79**, 6074 (1996).
- ¹⁶B. D. Cullity, *Elements of X-Ray Diffraction* (Addison-Wesley, Reading, MA, 1956), p. 388.
- ¹⁷S. Ino, *J. Phys. Soc. Jpn.* **21**, 346 (1966).
- ¹⁸S. Ino, *J. Phys. Soc. Jpn.* **27**, 941 (1969).
- ¹⁹J. W. Gibbs, in *Collected Works*, edited by W. R. Longley and R. G. van Name (Longmans and Green, New York, 1931); G. Wulff, *Z. Kristallogr.* **34**, 449 (1901).
- ²⁰C. Kittel, *Introduction to Solid State Physics*, 5th ed. (Wiley, New York, 1976), p. 74.
- ²¹P. R. Thornton and P. B. Hirsch, *Philos. Mag.* **3**, 738 (1958).
- ²²M. Alden, S. Mirbt, H. L. Skriver, N. M. Rosengaard, and B. Johansson, *Phys. Rev. B* **46**, 6303 (1992).
- ²³A. R. Miedema and B. E. Nieuwenhuys, *Surf. Sci.* **104**, 491 (1981).
- ²⁴L. Z. Mezey and J. Giber, *Jpn. J. Appl. Phys.* **21**, 1569 (1982).
- ²⁵*Handbook of Chemistry and Physics*, 66th ed., edited by C. Weast (CRC, Boca Raton, FL, 1987), D-43.
- ²⁶T. Ericsson, *Acta Metall.* **14**, 853 (1966).